MAX-PLANCK-INSTITUT FÜR PLASMAPHYSIK

GARCHING BEI MÜNCHEN

Localized Resistive Modes in the Circular Tokamak

D. Correa-Restrepo

IPP 6/240 August 1984

Die nachstehende Arbeit wurde im Rahmen des Vertrages zwischen dem Max-Planck-Institut für Plasmaphysik und der Europäischen Atomgemeinschaft über die Zusammenarbeit auf dem Gebiete der Plasmaphysik durchgeführt.

IPP 6/240 D. Correa-Restrepo Localized Resistive Modes in the Circular Tokamak

August 1984 (in English)

ABSTRACT

Localized resistive modes (resistive interchange and resistive ballooning modes) are investigated for self-consistent Tokamak equilibria which have circular cross-sections near the magnetic axis. The second region of stability (which is stable with respect to ideal ballooning modes at high poloidal beta β_p) proves to be unstable when resistive effects are taken into account as well. In the low β_p stability region, the stability boundaries are shifted toward lower β_p values. The magnitude of the shift depends on the degree of localization of the perturbation around the field line, highly localized perturbations being the most unstable ones. For negative values of β_p (pressure increasing outward) equilibria exist which are stable with respect to both ideal and resistive interchange and ballooning modes.

1. INTRODUCTION

IT has already been found that a plasma which is stable according to ideal MHD can be unstable if resistivity is also taken into account (see,for instance, FURTH et al., 1963; COPPIet al., 1966; GLASSER et al., 1975; CHANCE et al., 1978; STRAUSS, 1981; CORREA-RESTREPO, 1982, 1983.) One is therefore interested in knowing how the incorporation of resistivity into the MHD equations modifies the stability properties of a particular configuration.

In this paper, we evaluate the resistive ballooning mode criterion (which also describes ideal interchange and ballooning modes and resistive interchange instabilities) derived earlier (CORREA-RESTREPO, 1982, 1983) for a particular model of a tokamak, namely for self-consistent axisymmetric equilibria whose cross-sections are circular in the neighbourhood of the magnetic axis (LORTZ and NÜHRENBERG, 1979; ANTONSEN et al., 1982.) In this case, it is possible to find an analytical expression for the ballooning stability parameter Δ', which essentially depends on just the poloidal beta β_p, the shear parameter S, the safety factor on axis q_0 and the ratio ρ/R of the radius of the particular surface to the radius of the magnetic axis. For $q_0 = 1$, the different stability regions of this tokamak model are described by β_p and S alone.

An interesting result is that the second region of stability (which is stable at high β_p according to the ideal MHD theory) proves to be unstable when resistive effects are taken into account as well, because then resistive ballooning and inter change instabilities appear. The exact values of β_p at which the equilibria become unstable with respect to resistive interchanges depend weakly on whether one considers the stabil izing effect of finite plasma pressure or not (known in the literature as the cases of finite and large G, respectively). They are, however, always near the boundary for entering the second ideally stable region.

In the first region of stability, below the ideal ballooning stability limit, there are no resistive interchanges. However, resistive ballooning modes appear owing to destabilizing, large, positive values of the stability parameter Δ' . As a result, the stability boundaries are shifted toward lower values of β_p. The magnitude of the shift depends on the degree of localization of the perturbation around the field line, highly localized perturbations being the most unstable ones.

The situation is different for negative values of β_p , corresponding to a pressure increasing outward: here, equilibria exist which are stable with respect to both ideal and resistive modes.

Section 2 describes the equilibrium model. In Section 3, Δ' is calculated from the ideal ballooning mode equations. In Section 4, we study the stability with previously derived methods. In Section 5, the effect of q_0 on the stability is investigated.

The results are summarized in Section 6.

2. EQUILIBRIUM MODEL

The configurations treated here are self-consistent tokamak equilibria with circular cross-sections in the neighbourhood of the magnetic axis and are explained in some detail in the papers by LORTZ and NÜHRENBERG (1979) and by ANTONSEN et al. (1982).

We consider axisymmetric configurations, with a magnetic field given by

$$\vec{B} = \frac{1}{2\pi}\nabla\phi \times \nabla\chi + f\nabla\phi , \qquad (2.1)$$

$$B^2 = \frac{1}{4\pi^2 r^2} |\nabla\chi|^2 + f^2/r^2, \qquad (2.2)$$

where r and ϕ are coordinates of a cylindrical system r, ϕ, z (ϕ therefore being the toroidal angle about the axis of symmetry), χ is the poloidal magnetic flux and

$$f = (I_0 - I) / 2\pi , \qquad (2.3)$$

where I is the poloidal current and I_o is the total current flowing in the z-direction through a surface encircled by the magnetic axis.

To solve the equilibrium equation

$$\left(\frac{\partial^2}{\partial r^2} - \frac{1}{r}\frac{\partial}{\partial r} + \frac{\partial^2}{\partial z^2} \right) \chi + 4\pi^2 \left(r^2 \frac{dp}{d\chi} + f \frac{df}{d\chi} \right) = 0, \quad (2.4)$$

it is convenient to introduce coordinates ρ, θ by

$$r = R + \rho\cos\theta \quad , \quad z = \rho\sin\theta. \quad (2.5)$$

Then, ρ , θ are polar coordinates about $r = R$, $z = 0$, which is the magnetic axis.

Since we intend here to consider only configurations in which the magnetic surfaces are circular in the vicinity of the magnetic axis, the appropriate ansatz to solve equation (2.4) (LORTZ and NÜHRENBERG, 1979) is

$$f = f_0 + f_1\chi + \dots , \quad (2.6)$$

$$\frac{dp}{d\chi} = p_1 + \frac{p_2}{R^4}\chi + \dots, \quad (2.7)$$

$$\chi = \frac{\pi f_0}{q_0 R} \rho^2 + \chi_1(\theta)\rho^3 + \chi_2(\theta)\rho^4 + \ldots \quad (2.8)$$

The expansion coefficient f_1 is related to the value of the poloidal β , β_p , on the magnetic axis by

$$f_1 = (\beta_p - 1)/\pi q_0 R \; , \quad (2.9)$$

with q_o the safety factor on the magnetic axis.

The first terms (in an expansion in $\chi^{1/2}$) of the solution of the equilibrium equation yield

$$p_1 = - \frac{f_0}{\pi q_0} \frac{\beta_p}{R^3} \; , \quad (2.10)$$

$$\chi_1 = \frac{\pi f_0}{4 q_0 R^2} (1 + 4\beta_p)\cos\theta . \quad (2.11)$$

Here, the poloidal dependence of χ_1 has been chosen as $\cos\theta$.

3. CALCULATION OF Δ'

The investigation of the stability of a configuration with respect to resistive ballooning modes requires that Δ' be known. This quantity, described in detail by CORREA-RESTREPO (1982, 1983) must be evaluated from the asymptotic behaviour of the ideal, marginal ballooning mode equations for large values of the distance along the particular field line.

For a general equilibrium, Δ' must be calculated on any particular field line or, in our case of axisymmetric configurations, on any particular flux surfaca. Since we are interested here in the neighbourhood of the magnetic axis, we determine Δ' from the lowest-order solutions (in an expansion in $|\chi|^{1/2} \sim \rho/R$ of the marginal ideal ballooning mode equation

$$\frac{d}{dz}\{(1 + z^2)\frac{dF}{dz}\} + \{\frac{D_\infty}{4S^2} + \frac{\mu^2}{1 + z^2}\}F \quad , \qquad (3.1)$$

which was derived on the assumption that $q_0 = 1$ to satisfy Mercier's criterion on the axis (LORTZ and NÜHRENBERG, 1979; ANTONSEN et al., 1982.)
Here, S is the value of the shear on the magnetic axis, the shear being defined by

$$S(v) = 2\pi^2 R^3 \frac{\dot{q}}{q} \quad , \qquad (3.2)$$

with q the safety factor and the dot a derivative with respect to the volume v. Note that this definition of the shear differs from the usual one, namely $\sigma = (d\ln q/d\ln\rho)$. Near the axis one has

$$S = \frac{1}{2}\frac{R^2}{\rho^2}\sigma. \tag{3.3}$$

Thus, for a parabolic q-profile, σ vanishes as ρ^2 near the axis, while S remains finite.

For $q_0 = 1$, the quantities D_∞ and μ^2 only depend on β_p and S:

$$\frac{D_\infty}{4S^2} = -\frac{2\beta_p}{S} + \frac{3\beta_p}{64S^2}\{-1 + 2\beta_p - 48\beta_p^2 - 32\beta_p^3\}, \tag{3.4}$$

$$\mu^2 = \frac{\beta_p^2}{4S^2}\{32S - 24\beta_p^2 + 36\beta_p + 9\}. \tag{3.5}$$

To evaluate the resitive ballooning mode criterion, we shall also need a relation between the coordinate z which appears in equation (3.1) and the coordinate y used in the definition of Δ' (CORREA-RESTREPO, 1982):

$$z^2 = (\dot{q}^2 \dot{\chi}^2 |\nabla v|^4 / B^2) \; y^2 \; . \qquad (3.6)$$

We thus have near the magnetic axis

$$|z| = \left| \; 4\pi S \frac{\rho^2}{R^2} y \; \right| \; . \qquad (3.7)$$

The solutions of equation (3.1) are

$$F_+ = (1 + z^2)^{-\mu/2} \; F_1(a_1;b_1;c_1; -z^2) \quad \text{(even)} \quad (3.8)$$

and

$$F_- = z(1 + z^2)^{-\mu/2} \; F_1(a_2;b_2;c_2; -z^2) \quad \text{(odd)} \quad (3.9)$$

(ANTONSEN et al., 1982).

Here, the F_1's are hypergeometric functions and

$$a_1 = \frac{1 + s - \mu}{2} \; , \qquad (3.10)$$

$$b_1 = - \frac{(s + \mu)}{2} , \tag{3.11}$$

$$c_1 = 1/2 , \tag{3.12}$$

$$a_2 = \frac{2 + s - \mu}{2} , \tag{3.13}$$

$$b_2 = \frac{1 - s - \mu}{2} , \tag{3.14}$$

$$c_2 = 3/2 . \tag{3.15}$$

where

$$s = - \frac{1}{2} + \{ \frac{1}{4} - \frac{D_\infty}{4S^2} \}^{1/2} . \tag{3.16}$$

For large values of $|z|$, the asymptotic behaviour of the solutions F_+, F_- is given by

$$F_{\pm} (|z| \to \infty) \sim a_{1\pm} |z|^s + a_{2\pm} |z|^{-1-s} , \tag{3.17}$$

with

$$a_{1+} = \frac{\Gamma(c_1)\ \Gamma(a_1-b_1)}{\Gamma(a_1)\ \Gamma(c_1-b_1)} , \tag{3.18}$$

$$a_{2+} = \frac{\Gamma(c_1)\ \Gamma(b_1-a_1)}{\Gamma(b_1)\ \Gamma(c_1-a_1)} , \tag{3.19}$$

$$a_{1-} = \frac{\Gamma(c_2)\ \Gamma(a_2-b_2)}{\Gamma(a_2)\ \Gamma(c_2-b_2)} , \tag{3.20}$$

$$a_{2-} = \frac{\Gamma(c_2)\ \Gamma(b_2-a_2)}{\Gamma(b_2)\ \Gamma(c_2-a_2)} , \tag{3.21}$$

where the Γ's denote the gamma function. Taking into account equation (3.7) and the definition of Δ' given by CORREA-RESTREPO (1982), we finally obtain for even and odd modes, respectively

$$\Delta'_{+} = \left(\frac{R^2}{4\pi S\rho^2} \right)^{1+2s} \frac{\Gamma\{-\frac{(1+2s)}{2}\}\ \Gamma\{\frac{1+s-\mu}{2}\}\ \ \Gamma\{\frac{1+s+\mu}{2}\}}{\Gamma\{\ \frac{(1+2s)}{2}\}\ \Gamma\{\frac{-s-\ \mu}{2}\}\ \ \Gamma\{\frac{-s+\mu}{2}\}} , \tag{3.22}$$

$$\Delta'_{-} = \left(\frac{R^2}{4\pi S \rho^2} \right)^{1+2s} \frac{\Gamma\{-\frac{(1+2s)}{2}\} \; \Gamma\{\frac{1+(s-\mu)}{2}\} \; \Gamma\{\frac{1+(s+\mu)}{2}\}}{\Gamma\{\frac{(1+2s)}{2}\} \; \Gamma\{\frac{1-s-\mu}{2}\} \; \Gamma\{\frac{1-s+\mu}{2}\}} . \quad (3.23)$$

4. EVALUATON OF THE RESISTIVE BALLOONING MODE CRITERION

The evaluation of the resistive ballooning mode criterion (which also describes ideal interchange and ballooning modes and ideal interchange instabilities) involves the solution of a coupled system of two second-order ordinary differential equations on each closed field line (CORREA-RESTREPO, 1982; 1983). Straightforward numerical computations are difficult and lengthy in most practical cases, owing to the different length scales (time scales) which appear in the equations. However, by exploiting precisely this very aspect of the pro blem it is possible to simplify the calculations analytically: one is led to consider, not the full resistive ballooning mode equations, but two coupled, averaged equations in which the fast periodic poloidal variation has been eliminated. The stab ility ot the configuration can then be studied by solving these averaged equations with the appropriate boundary conditions. Neglecting the effect of compressibility in these equations (known in the literature as the case of large G, the quantity G being as defined in the appendix), it is possible to obtain a complete analytical solution and derive a dispersion relation

$\Delta' = \Delta(Q)$ for the growth rate Q. Evaluating this dispersion relation naively leads to instability whenever Δ' is positive. However, as pointed out by CORREA-RESTREPO (1982, 1983) , in the low β_p region, which is stable with respect to both ideal ballooning and resistive interchange modes, only positive Δ' values above a critical Δ_{crit} lead to results which are consistent with the restrictions of the theory. Below Δ_{crit}, the growth rates are so small (they are proportional to the resistivity instead of to a fractional power of it) that they violate previously imposed conditions.

A critical value of Δ' also arises -in a more natural way- if one takes the effect of finite G into account. This has been shown explicitly (CONNOR et al., 1983) for the case of a standard tokamak (which can be obtained as a particular case of our model if we choose $S \sim 1/\varepsilon_a^2$, i.e. $D_R \sim \varepsilon_a^2$, D_R being the resistive interchange stability parameter, which is given explicitly in the appendix, $\beta_p \sim 1$. $\varepsilon_a = a/R$ is the inverse aspect ratio). In this case of finite G, Δ_{crit} is the value of Δ' above which the real part of the (complex) growth rate becomes positive. Here, for simplicity, we make the calculations with the expression for Δ' derived for the case of large G. This does not affect the general features of the results, namely that new instabilities appear in the ideal ballooning and resistive interchange stable regions. Also, instead of the low-β_p , ideal MHD stability limit, new stability boundaries are found at lower β_p values.

In the appendix, we derive the equilibrium quantities M, G, H, D_R and the scale factor y_o , which enter the stability criterion (CORREA-RESTREPO, 1982; 1983).

We first recall the ideal stability calculations. From equations (3.16) and (3.17) one easily sees that Mercier's stability boundaries are given by

$$s^2 - D_\infty = 0 , \qquad (4.1)$$

where Mercier's exponent s changes from real to complex values. The Mercier unstable region is shown in Figs. 1 - 5 .
In particular, configurations with both S and β_p positive are Mercier stable.

The ideal ballooning stability boundaries are obtained when the coefficient of the large solutions in equation (3.17) vanishes and Δ' jumps from $-\infty$ to $+\infty$:

$$\frac{1 + s - \mu}{2} = - m, \quad m= 0, 1, 2... \text{ (even modes)}, \qquad (4.2)$$

$$1 + \frac{s - \mu}{2} = - m, \quad m= 0, 1, 2... \text{ (odd modes)}. \qquad (4.3)$$

The stability boundaries for the most unstable mode (m = 0, even) are displayed in Figs. 1 - 4.

We now study the resistive interchanges. Taking into account the effect of compressibility (finite G), the con dition for instability with respect to resistive inter changes is

$$D_R > \frac{(1 + 2\nu)^2}{G}, \qquad \nu = 0, 1, 2... \qquad (4.4)$$

(CORREA-RESTREPO, 1982). For $G^{-1} = 0$ one obtains the well known stability boundary $D_R = 0$. This is shown in Fig. 2. For large values of β_p and S, the curve $D_R = 0$ and the upper ideal ballooning stability boundary coincide, a feature which cannot be seen in Fig. 2. The ideally stable second region of stability is almost completely destroyed by the appearance of resistive interchange modes. If the stabilizing effect of finite G is taken into account, the limit for entering the resistive interchange unstable region is shifted toward higher values of β_p . This, however, is a small effect, as can be seen in Fig. 3 for the most unstable mode ($\nu = 0$) and for different values of the inverse aspect ratio ε_a , corresponding to different values of G. The narrow band between the upper ideal ballooning stability boundary and the curves $D_R = G^{-1}$, though stable with respect to ideal ballooning and resistive interchange modes, is unstable with respect to resistive ballooning modes.

It should be mentioned that in order to determine the growth rates of resistive ballooning modes when $D_R < 0$ and $s > 1/2$, the simple dispersion relation $\Delta' = \Delta(Q)$, where Δ' is obtained from the ideal marginal equation as described above, does not hold. In this case, Δ' cannot be determined from the lowest-order ballooning mode equations alone (in an expansion with respect to small resistivity and and inertia), it being necessary to include further terms in the inner expansion, up to terms of order δ^n, $n \leq (1 + 2s)/2$, δ being a small expansion parameter defined elsewhere (CORREA-RESTREPO, 1982, equation (69)). Here, we do not treat this problem in further detail.

When $s < 1/2$ and $D_R < 0$ (which is everywhere the case in the low-β_p, ideally stable region in Figs. 1 - 4, the condition for instability with respect to resistive ballooning modes is

$$\Delta' > \Delta_{crit} \tag{4.5}$$

with

$$\Delta_{crit} = \frac{4}{\pi} (\cos\frac{\pi s}{2}) (\frac{1}{2} + s) \Gamma^2 (\frac{1}{2} + s) \frac{Q_{crit}^{(5-2s)/4}}{(1+s-H)^2 - Q_{crit}^3} .$$

$$\frac{\Gamma\{ \frac{1}{4}(Q_{crit}^{3/2} + 3 - 2s + |D_R|/Q_{crit}^{3/2}) \}}{\Gamma\{ \frac{1}{4}(Q_{crit}^{3/2} + 1 + 2s + |D_R|/Q_{crit}^{3/2}) \}} \; y_0^{(1+2s)}, \qquad (4.6)$$

$$Q_{crit}^{3/2} = |D_R|/4 \qquad (4.7)$$

(CORREA-RESTREPO, 1982; 1983). The scale factor y_0 is given in detail in the appendix and depends on the shear S, the the aspect ratio ε_a^{-1} , the ratio of the resistive diffusion time to Alfvén transit time τ_R/τ_A , the mode number $k_\perp^2$ and the relative radius ρ/a of the particular surface, which is assumed to be located in the neighbourhood of the magnetic axis, i. e., we assume $\rho/a \ll 1$. Figure 4 shows the stability boundaries obtained with different values of these parameters. The curves are the loci of the points $\Delta'(S,\beta_p) = \Delta_{crit}$ and represent an stability boundary in the sense described in detail at the beginning of this section.

In order to get an idea of the magnitude of the growth rates of the resistive modes, we have plotted in Fig. 5 the normalized growth rate

$$\bar{\gamma} = \{ \frac{\gamma}{\omega_A} \frac{2\pi M^{1/2} R^2}{4\pi S \rho^2} \} \tag{4.8}$$

as a function of β_p for a fixed value of the shear (S = 25).

In the region of negative shear and negative β_p (pressure decreasing outward), there is a region of negative D_R values which is stable to all the modes considered here.

5. THE $q_0 \neq 1$ CASE

In the previous sections we have considered the somewhat singular situation in which the safety factor on the magnetic axis is equal to unity. When $q_0 \neq 1$, the quantity D_R, which is crucial for both ideal and resistive stability, behaves in a substantially different way in the neighbourhood of the magnetic axis. This can immediately be seen when D_R is derived for the case $q_0 \neq 1$. Then, instead of equation (A.17), one obtains

$$D_R = D_R(q_0 = 1) - \frac{\beta_p (q_0^2 - 1)}{S^2 q_0^2 \rho^2 / R^2} , \tag{5.1}$$

with $D_R(q_0 = 1)$ given by equation (A.17).

If $q_0 < 1$, D_R diverges and is positive when one approaches the magnetic axis. The neighbourhood of the axis is then Mercier unstable. We do not look further into this case.

If $q_0 > 1$, D_R has a strong stabilizing effect, since it becomes large and negative as one approaches the magnetic axis, whose immediate neighbourhood is then stable. However, as one proceeds from the axis outwards, this stabilizing effect is reduced and one eventually enters an unstable region. To study the stability in such a situation one has to include the effect of the new terms in D_R and obtains

$$\frac{d}{dz}(1 + z^2)\frac{dF}{dz} + \left\{ \frac{\mu^2}{1 + z^2} + \frac{D_\infty}{4S^2} - \frac{\beta_p (q_0^2 - 1) R^2}{S^2 q_0^2 \rho^2} \right\} F, \quad (5.2)$$

instead of equation (3.1). The stability of the system can be studied with exactly the same methods as before. It is clear that Δ' now has an additional dependence on q_0 and R^2/ρ^2 . For a particular case ($q_0 = 1.05$, $\rho/R = 0.1$), the results are illustrated in Fig. 5 : in the range of positive β_p values, the region of instability with respect to ideal ballooning modes is reduced. Also, the boundaries for the onset of resistive interchanges are shifted toward higher values of β_p . The stability boundaries for resistive ballooning modes are illustrated in Fig. 7 for a particular value of the shear ($S = 25$) and different values of τ_R/τ_A and $k_\perp$.

6. SUMMARY

We have studied some effects of resistivity on the stability of tokamak equilibria which have circular cross-sections near the magnetic axis. For these configurations, the ideal MHD ballooning mode theory predicts a second region of stability at high values of β_p . These good stability propertities at high β_p deteriorate in the presence of resistivity, which introduces both resistive interchange and resistive ballooning modes.

In the first region of (ideal) stability, no resistive interchanges appear. Here, however, resistive ballooning modes shift the stability boundaries toward lower values of β_p , the magnitude of the shift depending on the degree of localization of the perturbation. If one allows arbitrarily large mode numbers (corresponding to very localized perturbations in our picture), the whole region of stability would be destroyed. This, however, would not be consistent with the model employed, finite Larmor radius effects having to be taken into account.

REFERENCES

ANTONSEN, JR. T. M., FERREIRA A. and RAMOS J.J. (1982) Plasma Physics 24 , 197.

CHANCE M. S., DEWAR R.L., FRIEMAN E. A., GLASSER J. M., GRIMM R. C., JARDIN S. C., JOHNSON J. L., MANICKAM J., OKABAYASHI M. and TODD A. M. M. (1978) In Plasma Physics and Controlled Nuclear Fusion Research, Vol I, p. 677. International Atomic Energy Agency, Vienna.

COPPI B., GREENE J.M. and JOHNSON J. L. (1966) Nucl. Fusion 6, 101.

CONNOR, J. W., HASTIE R. J., MARTIN T. J., SYKES A. and TURNER M. F. (1983) In Plasma Physics and Controlled Nuclear Fusion Research 1982, Vol III, p. 403. International Atomic Energy Agency, Vienna.

CORREA-RESTREPO D. (1982) Z. Naturforsch. 37 a, 848.

CORREA-RESTREPO D. (1983) In Plasma Physics and Controlled Nuclear Fusion Research 1982, Vol III, p.519. International Atomic Energy Agency, Vienna.

FURTH H. P., KILLEEN J. and ROSENBLUTH M. N. (1963) Phys. Fluids 6, 459.

GLASSER A. H., GREENE J. M. and JOHNSON J. L. (1975) Phys. Fluids 18 , 875.

LORTZ D. and NÜHRENBERG J. (1979) Nucl. Fusion 19 , 1207.

STRAUSS H. R. (1981) Phys. Fluids 24 , 2004.

APPENDIX

CALCULATION OF THE EQUILIBRIUM QUANTITIES AND SCALE FACTOR NEEDED TO EVALUATE THE RESISTIVE BALLOONING MODE CRITERION

In the axisymmetric case, the equilibrium quantities M, G and H can be expressed as

$$M = \langle B^2/|\nabla\chi|^2\rangle \{ \langle|\nabla\chi|^2/B^2\rangle + 4\pi^2 f^2 (\langle B^{-2}\rangle - \langle B^2\rangle^{-1}) \}, \qquad (A.1)$$

$$G = \langle B^2\rangle/\gamma_H p M, \qquad (A.2)$$

$$H = \frac{2\pi f}{\dot{q}} \frac{dp}{d\chi} \{ \langle 1/|\nabla\chi|^2\rangle - \frac{\langle B^2/|\nabla\chi|^2\rangle}{\langle B^2\rangle} \}. \qquad (A.3)$$

In order to calculate the mean values, it is convenient to invert the power series for $\chi(\rho,\theta)$, equation (2.8) and express ρ as a function of χ and θ :

$$\rho(\chi,\theta) = (\chi/\chi_0)^{1/2} \{ 1 - \frac{\chi_1(\theta)}{2\chi_0} (\chi/\chi_0)^{1/2} + \qquad (A.4)$$

$$\rho_2(\theta)(\chi/\chi_0) + \dots \},$$

where $\chi_0 = \pi f_0/q_0 R$.

Taking into account equations (2.2) and (2.6) - (2.11), one then obtains

$$B^2 = \frac{f_0^2}{R^2}\{ 1 - \frac{2\cos\theta}{R} (\chi/\chi_0)^{1/2} + \{ (\cos\theta\ \chi_1(\theta))/(R\ \chi_0) + (3\cos^2\theta/R^2 + (\chi_0^2/\pi^2 f_0^2) + (2f_1\chi_0/f_0\}(\chi/\chi_0) + \ldots \} , \tag{A.5}$$

$$|\nabla\chi|^2 = 4\chi_0\chi\ \{ 1 + (2\chi_1(\theta)/\chi_0)\ (\chi/\chi_0)^{1/2} + \{ 2\rho_2(\theta) - 2(\chi_1^2(\theta)/\chi_0^2) + (\chi_1'^2(\theta)/4\chi_0^2 + 4\chi_2(\theta)/\chi_0\}\ (\chi/\chi_0) + \ldots \} , \tag{A.6}$$

which lead to the following surface mean values:

$$\langle B^2\rangle = \frac{f_0^2}{R^2}\{ 1 + \{ \frac{\langle\cos\theta\ \chi_1\rangle}{R\chi_0} + \frac{3}{2R^2} + \frac{\chi_0^2}{\pi^2 f_0^2} + \frac{2f_1\chi_0}{f_0}\} \frac{\chi}{\chi_0} + \ldots \} , \tag{A.7}$$

$$\frac{1}{<B^2>} = \frac{R^2}{f_0^2} \{ 1 - \{ \frac{<\cos\theta\ \chi_1>}{R\chi_0} + \frac{3}{2R^2} + \frac{\chi_0^2}{\pi^2 f_0^2} + \frac{2f_1\chi_0}{f_0} \} \frac{\chi}{\chi_0} + \ldots \} , \qquad (A.8)$$

$$< \frac{1}{B^2} > = \frac{R^2}{f_0^2} \{ 1 + \{ \frac{1}{2R^2} - \frac{<\cos\theta\ \chi_1>}{R\chi_0} - \frac{\chi_0^2}{\pi^2 f_0^2} - \frac{2f_1\chi_0}{f_0} \} \frac{\chi}{\chi_0} + \ldots \} , \qquad (A.9)$$

$$< \frac{B^2}{|\nabla\chi|^2} > = \frac{f_0^2}{4\chi_0\chi R^2} \{ 1 + \{ \frac{<5\cos\theta\ \chi_1>}{R\chi_0} + \frac{3}{2R^2} + \frac{\chi_0^2}{\pi^2 f_0^2} +$$

$$\frac{2f_1\chi_0}{f_0} - 2<\rho_2> + \frac{23}{4} \frac{<\chi_1^2>}{\chi_0^2} - \frac{<4\chi_2>}{\chi_0} \} \frac{\chi}{\chi_0} + \ldots \} , \qquad (A.10)$$

$$< \frac{|\nabla\chi|^2}{B^2} > = \frac{4\chi_0\chi R^2}{f_0^2} \{ 1 + \{ \frac{<3\cos\theta\ \chi_1>}{R\chi_0} + \frac{1}{2R^2} - \frac{\chi_0^2}{\pi^2 f_0^2} -$$

$$\frac{2f_1\chi_0}{f_0} + 2<\rho_2> - \frac{7}{4} \frac{<\chi_1^2>}{\chi_0^2} + \frac{<4\chi_2>}{\chi_0} \} \frac{\chi}{\chi_0} + \ldots \} . \qquad (A.11)$$

With these expressions we obtain (to lowest order in $\chi \sim \rho^2/R^2$)

$$M = 1 + 2q_0^2 , \tag{A.12}$$

$$H = \frac{2\beta_p}{S} \left(\beta_p + \frac{1}{4} \right), \tag{A.13}$$

$$G = \frac{3}{5} \cdot \frac{1}{M\beta_p} \cdot \frac{q_0^2 R^2}{a^2} . \tag{A.14}$$

In deriving the last expression we set $\gamma_H = 5/3$ and defined the radius a by

$$\frac{p(0)}{\langle B^2\rangle(0)} = \frac{\beta_p a^2}{q_0^2 R^2} . \tag{A.15}$$

The remaining equilibrium quantity which enters the stability criterion, namely D_R, can be derived from H and $D_\infty/4S^2$, equation (3.4), by means of the relation

$$D_R = H^2 - H + \frac{D_\infty}{4S^2} , \tag{A.16}$$

which follows from the definitions of D_R and $D_\infty/4S^2$. This leads to

$$D_R = \frac{\beta_p}{32S^2} \{ -64(\beta_p + \frac{5}{4})S - \frac{3}{2} + 11 {}_p - 8\beta_p^2 + 80\beta_p^3 \} . \qquad (A.17)$$

This expression for D_R is valid only when $q_0 = 1$. When $q_0 \neq 1$, terms proportional to $(q_0^2 - 1)\cdot(R^2/\rho^2)$ must be taken into account.

Besides the equilibrium quantities, the scale factor y_0 (CORREA-RESTREPO 1982, 1983) must also be evaluated. This is given by

$$y_0 = \{ \frac{\langle B^2/|\nabla\chi|^2\rangle \ |\dot{\chi}|^3}{\langle B^2\rangle \ \rho_{pl}^{1/2} \ k_\perp^2\eta \ \dot{q}^2 \ M^{1/2}} \}^{1/3} , \qquad (A.18)$$

with ρ_{pl} the plasma density, η the resistivity and $1/k_\perp$ a small number which defines the degree of localization of the perturbation around the field line.
Defining the Alfvén transit time by $\tau_A = \rho_{pl}^{1/2} \ qR \ / \ \langle B^2\rangle$ and the resistive diffusion time by $\tau_R = 4\pi^2 a^2/\eta$ (with a from equation (A.15)), one then obtains

$$y_0 = (\frac{R^2}{4\pi S \ \rho^2}) . \{ 2S \ \frac{a^2}{R^2} \ \frac{\tau_R}{\tau_A \ k_\perp^2} \ \frac{1}{(1 + 2q_0^2)^{1/2}} \}^{1/3} .$$

$$(\frac{\rho}{R})^{4/3} . \qquad (A.19)$$

FIGURE CAPTIONS

FIG.1 Stability boundaries for ideal interchange and ballooning modes.

FIG.2 Stability boundaries ($D_R = 0$) for resistive interchange modes.

FIG.3 Stabilizing effect of compressibility (finite G^{-1}) on the stability of resistive interchange modes. Given ε_a , the fastest growing resistive interchange mode is unstable if $D_R > G^{-1}(\varepsilon_a)$. The curves labeled 1, 2, 3 are for $\varepsilon_a = 0$, 0.1 and 0.25, respectively.

FIG.4 Stability boundaries for resistive ballooning modes. The relevant parameters are clearly given in the diagram.

FIG.5 Stabilizing effect of $q_0 > 1$. Shown in the diagram are the stability boundaries for ideal and resistive interchanges and ideal ballooning modes.

FIG.6 Normalized growth rates $\bar{\gamma}$ of ideal and resistive ballooning modes for $q_0 = 1$, $S = 25$ and different values of τ_R/τ_A and $k_\perp$. The values of β_p corresponding to the condition (4.5) are clearly indicated by the arrows.

FIG.7 Normalized growth rate $\bar{\gamma}$ of ideal and resistive ballooning modes for $q_0 = 1.05$, $S = 25$, $\rho/R = 0.1$ and different values of $k_\perp$.

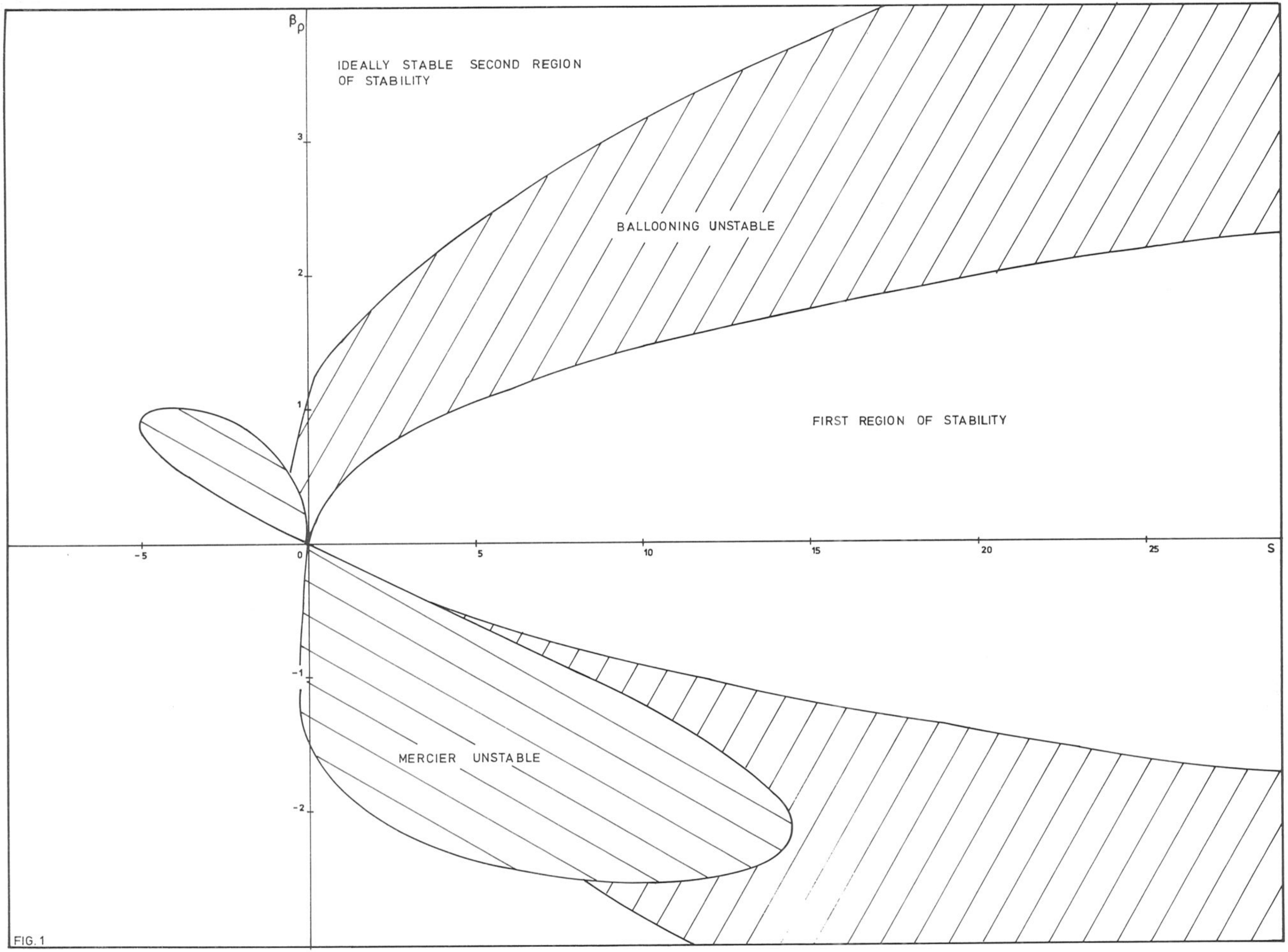

β_ρ
IDEALLY STABLE SECOND REGION OF STABILITY
BALLOONING UNSTABLE
FIRST REGION OF STABILITY
MERCIER UNSTABLE
S
-5
0
5
10
15
20
25
3
2
1
-1
-2

FIG. 1

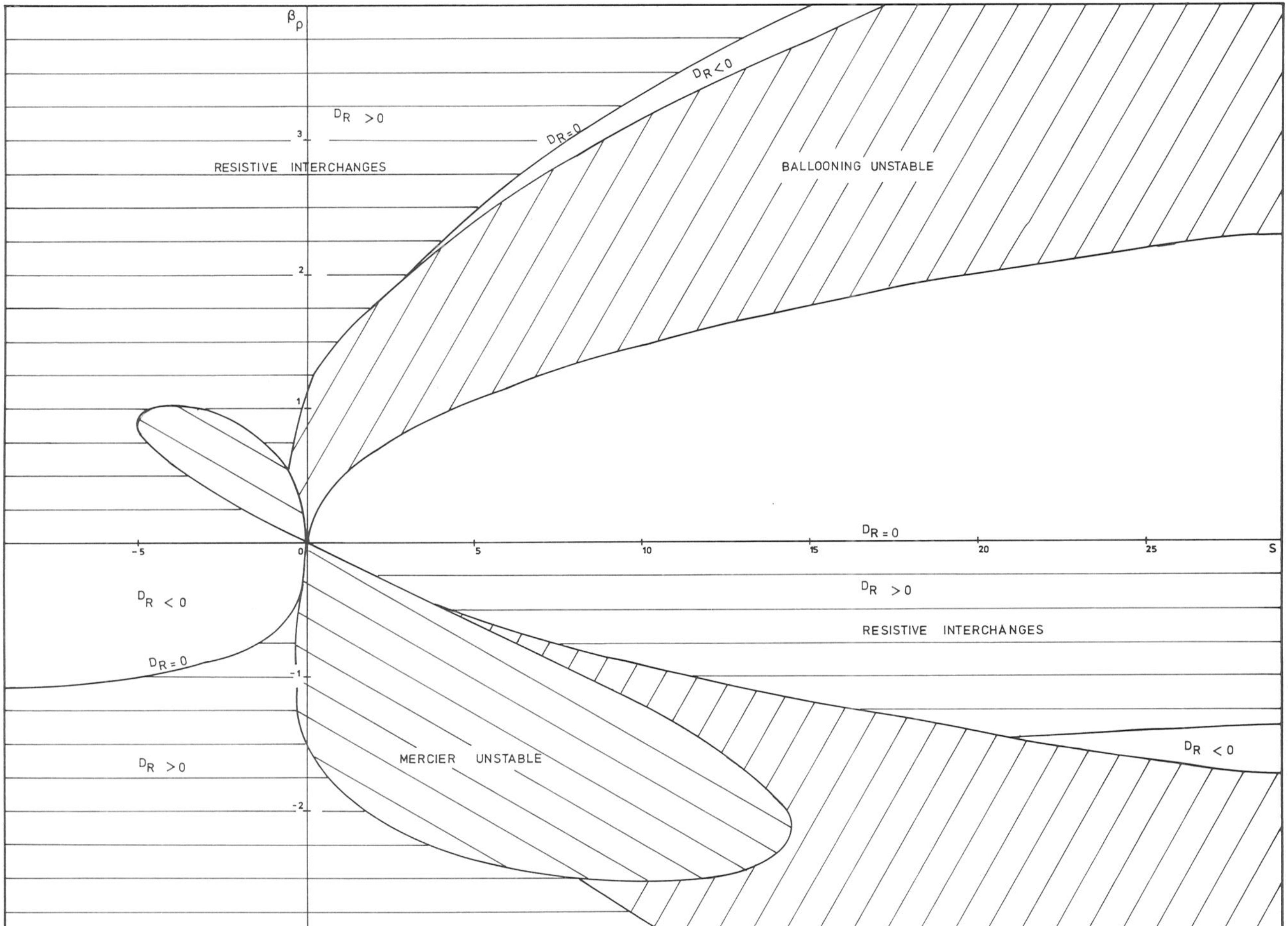
β_ρ
D_R < 0
D_R = 0
D_R > 0
3
2
1
0
-1
-2
-5
5
10
15
20
25
S
RESISTIVE INTERCHANGES
BALLOONING UNSTABLE
D_R = 0
D_R > 0
RESISTIVE INTERCHANGES
D_R < 0
D_R = 0
D_R > 0
MERCIER UNSTABLE
D_R < 0

FIG. 2

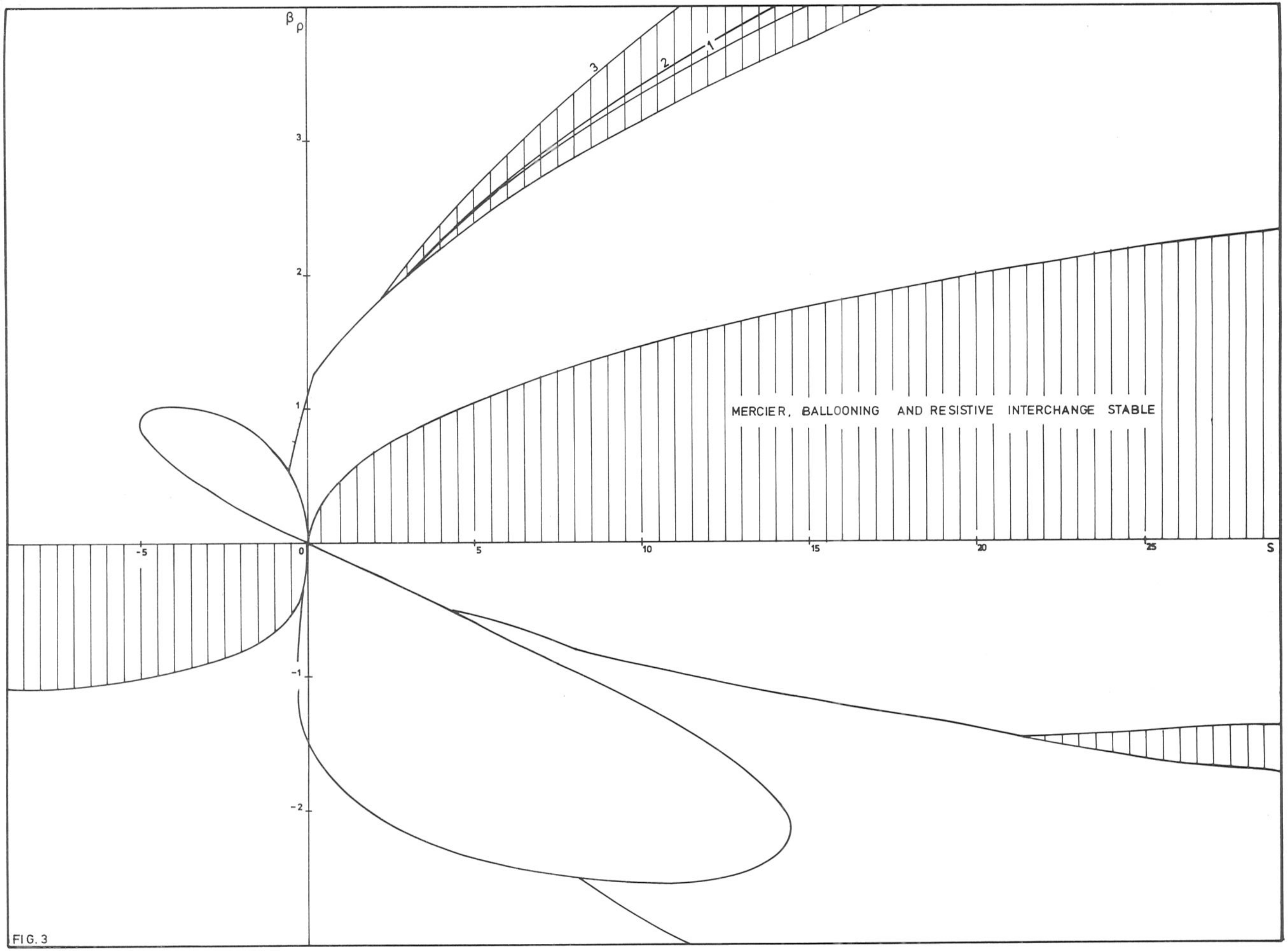

β_ρ
3
2
1
0
-1
-2
-5
5
10
15
20
25
S
1
2
3
MERCIER, BALLOONING AND RESISTIVE INTERCHANGE STABLE

FIG. 3

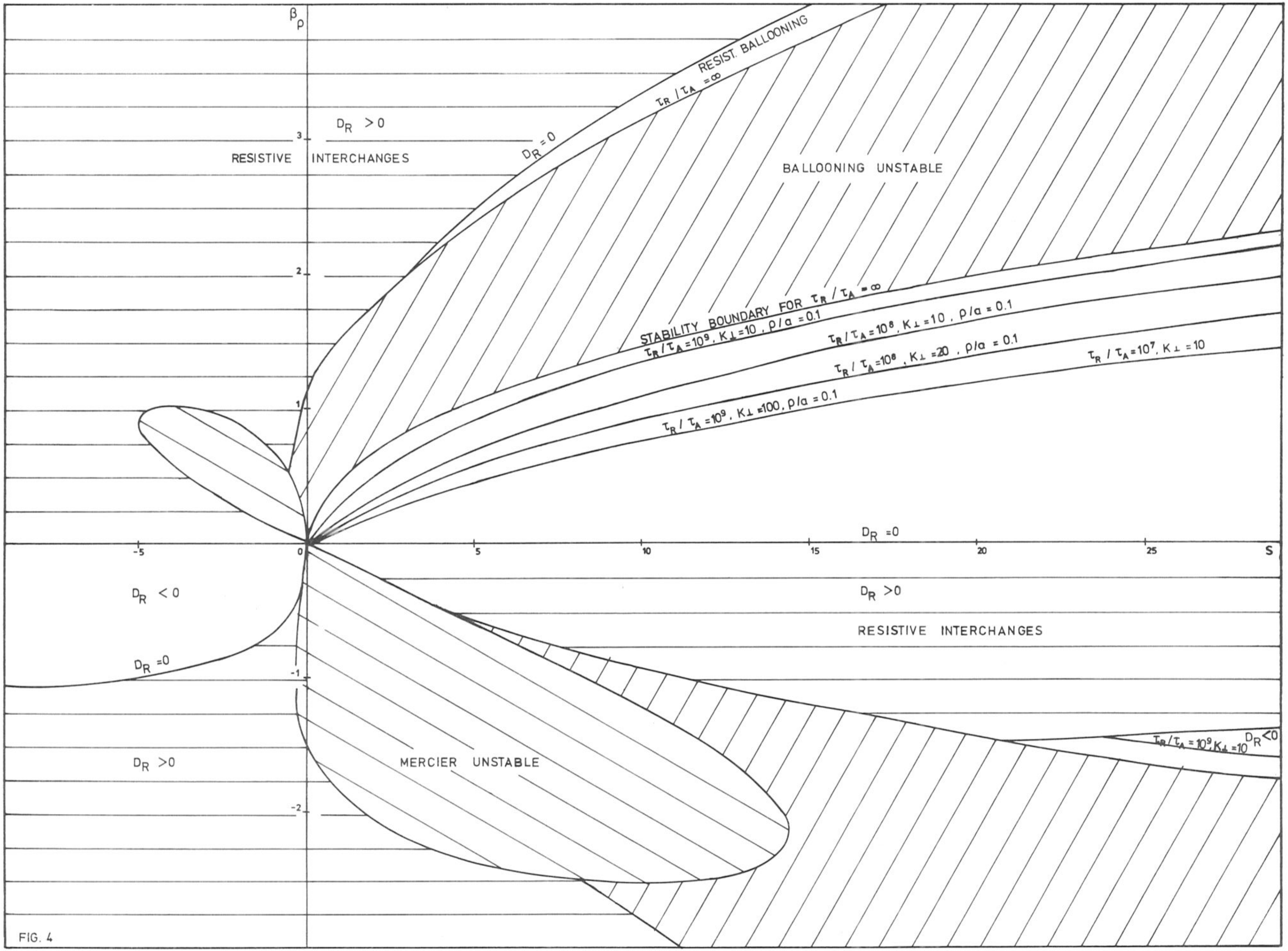

β_p
S
RESISTIVE INTERCHANGES
$D_R > 0$
$D_R = 0$
$D_R < 0$
$D_R > 0$
RESIST. BALLOONING
$\tau_R / \tau_A = \infty$
BALLOONING UNSTABLE
STABILITY BOUNDARY FOR $\tau_R / \tau_A = \infty$
$\tau_R / \tau_A = 10^9$, $K_\perp = 10$, $\rho/a = 0.1$
$\tau_R / \tau_A = 10^8$, $K_\perp = 10$, $\rho/a = 0.1$
$\tau_R / \tau_A = 10^8$, $K_\perp = 20$, $\rho/a = 0.1$
$\tau_R / \tau_A = 10^7$, $K_\perp = 10$
$\tau_R / \tau_A = 10^9$, $K_\perp = 100$, $\rho/a = 0.1$
$D_R = 0$
$D_R > 0$
RESISTIVE INTERCHANGES
$\tau_R / \tau_A = 10^9$, $K_\perp = 10$
$D_R < 0$
MERCIER UNSTABLE

FIG. 4

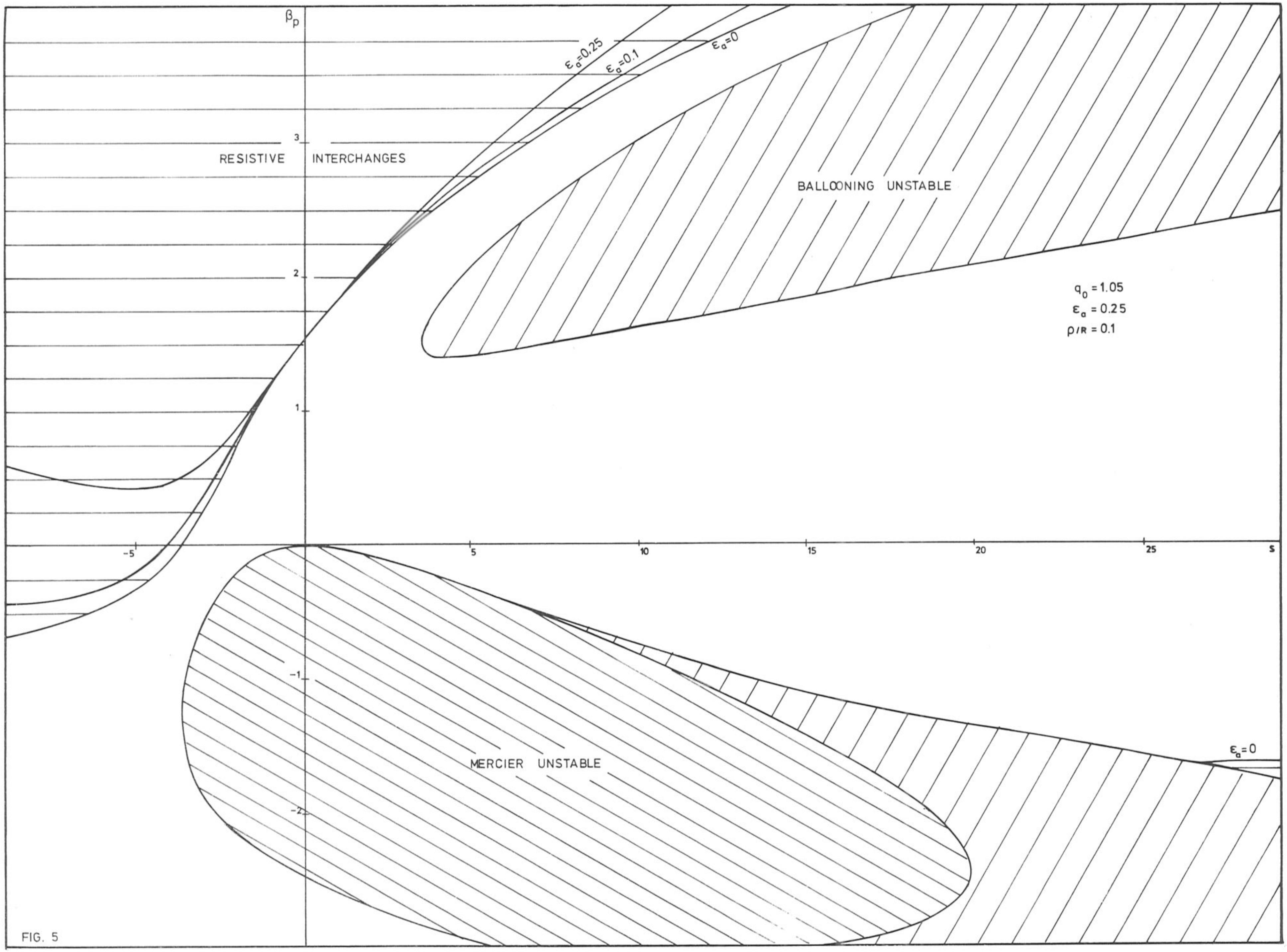

β_p
RESISTIVE INTERCHANGES
BALLOONING UNSTABLE
MERCIER UNSTABLE
$\varepsilon_a = 0.25$
$\varepsilon_a = 0.1$
$\varepsilon_a = 0$
$q_0 = 1.05$
$\varepsilon_a = 0.25$
$\rho / R = 0.1$
-5
5
10
15
20
25
s
3
2
1
-1
-2

FIG. 5

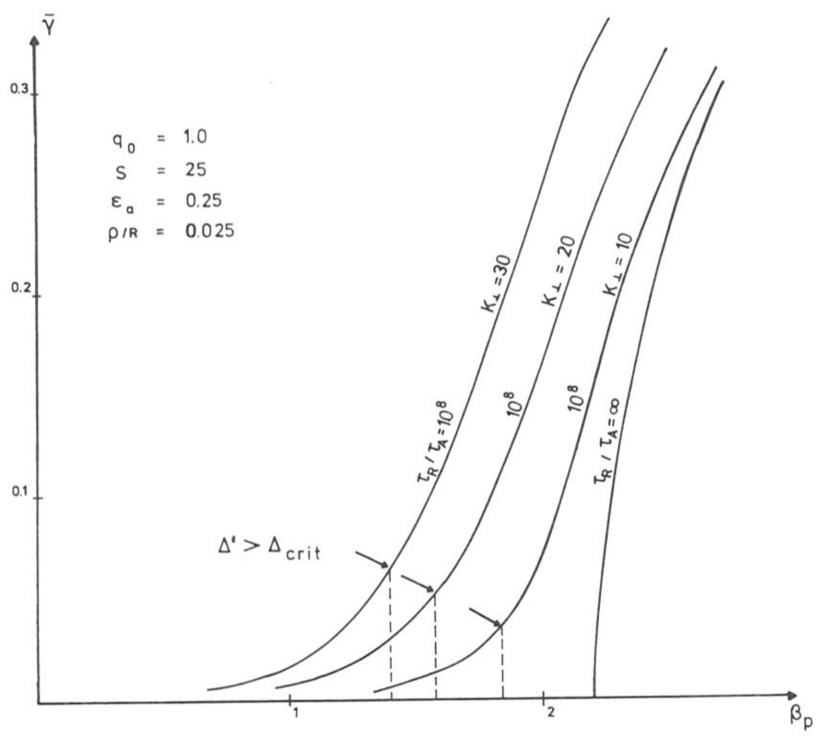

$\bar{\gamma}$
0.3
0.2
0.1
$q_0 = 1.0$
$S = 25$
$\varepsilon_a = 0.25$
$\rho/R = 0.025$
$K_\perp = 30$
$K_\perp = 20$
$K_\perp = 10$
$\tau_R/\tau_A = 10^8$
10^8
10^8
$\tau_R/\tau_A = \infty$
$\Delta' > \Delta_{crit}$
1
2
β_p

FIG. 6

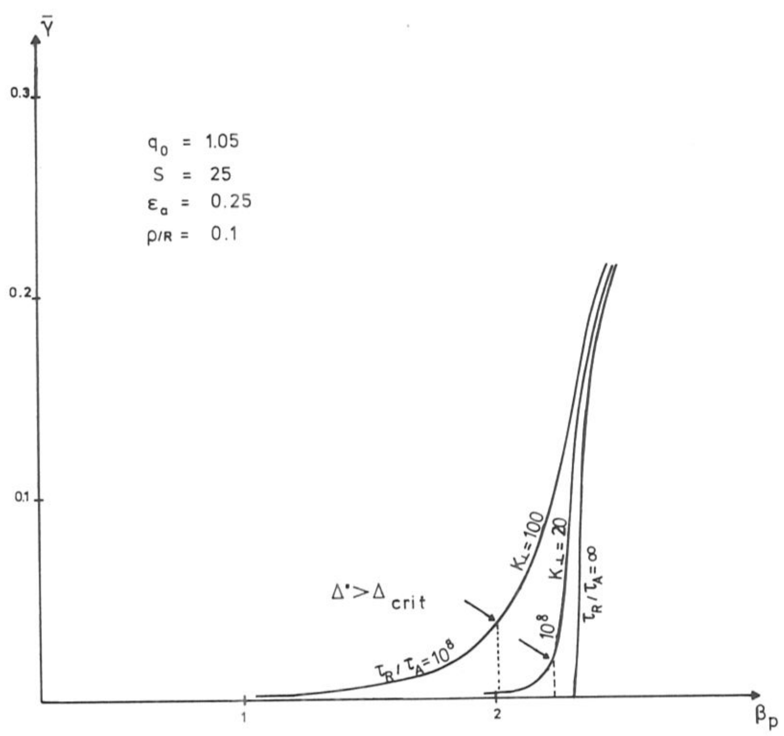

$\bar{\gamma}$
0.3
0.2
0.1
$q_0 = 1.05$
$S = 25$
$\varepsilon_a = 0.25$
$\rho/R = 0.1$
$K_\perp = 100$
$K_\perp = 20$
$\tau_R/\tau_A = \infty$
$\Delta' > \Delta_{crit}$
$\tau_R/\tau_A = 10^8$
10^8
1
2
β_p

FIG. 7